19. Fischer K-D. *et al.* Vav is a regulator of cytoskeletal reorganization mediated by the T-cell receptor. *Curr. Biol.* **8,** 554–562 (1998).
20. Holsinger L. J. *et al.* Defects in actin-cap formation in Vav-deficient mice implicate an actin requirement for lymphocyte signal transduction. *Curr. Biol.* **8,** 563–572 (1998).
21. Zhang, A., Alt, F. W., Davidson, L., Orkin, S. H. & Swat, W. Defective signaling through T- and B-cell antigen receptors in lymphoid cells lacking the vav proto-oncogene. *Nature* **374,** 470–473 (1995).
22. Tarakhovsky, A. *et al.* Defective antigen receptor-mediated proliferation of B and T cells in the absence of Vav. *Nature* **374,** 467–470 (1995).
23. Fischer, K. D. *et al.* Defective T-cell receptor signalling and positive selection of vav-deficient $CD4^+CD8^+$ thymocytes. *Nature* **374,** 474–477 (1995).
24. Wu, J., Motto, D. G., Koretzky, G. A. & Weiss, A. Vav and SLP-76 interact and functionally cooperate in IL-2 gene activation. *Immunity* **4,** 593–602 (1996).
25. Segal, B. M., Dwyer, B. K. & Shevach, E. M. An interleukin (IL)-10/IL-12 immunoregulatory circuit controls susceptibility to autoimmune disease. *J. Exp. Med.* **187,** 537–546 (1998).
26. Hardt, W. -D., Chen, L. M., Schuebel, K. E., Bustelo, X. R. & Galan, J. E. S. typhimurium encodes an activator of Rho GTPase that induces membrane ruffling and nuclear responses in host cells. *Cell* **93,** 815–826 (1998).

Supplementary information is available on *Nature*'s World-Wide Web site (http://www.nature.com) or as paper copy from the London editorial office of *Nature*.

Acknowledgements

We thank L. X. Zheng, Y. C. Liu and Y. Pewzner-Jung for the reagents, and K. Druey, D. Garboczi, R. N. Germain, W. E. Paul and R. H. Schwartz for critical comments on the manuscript.

Correspondence and requests for materials should be addressed to H.G. (e-mail: hgu@niaid.nih.gov).

Measurement of thermal contribution to photoreceptor sensitivity

Ari Koskelainen*, Petri Ala-Laurila*, Nanna Fyhrquist† & Kristian Donner†

* *Laboratory of Biomedical Engineering, PO Box 2200, Helsinki University of Technology, FIN-02015 HUT, Finland*
† *Department of Biosciences, Division of Animal Physiology, FIN-00014 University of Helsinki, Finland*

Activation of a visual pigment molecule to initiate phototransduction requires a minimum energy, E_a, that need not be wholly derived from a photon, but may be supplemented by heat[1]. Theory[2,3] predicts that absorbance at very long wavelengths declines with the fraction of molecules that have a sufficient complement of thermal energy, and that E_a is inversely related to the wavelength of maximum absorbance (λ_{max}) of the pigment. Consistent with the first of these predictions, warming increases relative visual sensitivity to long wavelengths[4–8]. Here we measure this effect in amphibian photoreceptors with different pigments to estimate E_a (refs 2, 5–7) and test experimentally the predictions of an inverse relation between E_a and λ_{max}. For rods and 'red' cones in the adult frog retina, we find no significant difference in E_a between the two pigments involved, although their λ_{max} values are very different. We also determined E_a for the rhodopsin in toad retinal rods—spectrally similar to frog rhodopsin but differing in amino-acid sequence—and found that it was significantly higher. In addition, we estimated E_a for two pigments whose λ_{max} difference was due only to a chromophore difference (A1 and A2 pigment, in adult and larval frog cones). Here E_a for A2 was lower than for A1. Our results refute the idea of a necessary relation between λ_{max} and E_a, but show that the A1 → A2 chromophore substitution decreases E_a.

Phototransduction is initiated when a molecule of visual pigment absorbs a photon of sufficient energy to isomerize the chromophore. Stiles[2] suggested that the energy barrier for pigment activation (E_a) does not set a sharp minimum requirement on photon energy (hc/λ), because part of the total energy can be drawn from appropriate vibrational modes of the molecule[6]. If this were not the case, every visual pigment would have a limiting wavelength $\lambda_a = hc/E_a$ where absorbance (or visual sensitivity) drops precipitously to zero, whereas all spectra in fact show a continuous, smooth decline. When plotted on logarithmic ordinates against $1/\lambda$ (thus photon energy), the decline follows a straight line at the longest wavelengths for as far as absorbance or sensitivity can be measured. This is predicted on the basis of classical statistical physics, if the probability that low-energy photons produce isomerizations is proportional to the cumulative distribution of pigment molecules on thermal energy levels greater than $E_a - hc/\lambda$. One corollary is that absorbances/sensitivities at long wavelengths ($\lambda > \lambda_a$) should be relatively increased by warming, which has indeed been observed in psychophysical[4,6], behavioural[5] and electrophysiological[7,8] measurements. The theory permits calculation of E_a from the size of the temperature effect at any wavelength $\lambda > \lambda_a$: the effect is translated into equivalent photon energy via the local slope of the sensitivity spectrum on a $1/\lambda$ abscissa (see equation (1) in Methods)[4–7].

We use this method to estimate E_a for spectrally different and spectrally similar visual pigments. The purpose is to test the idea of a straightforward relation between spectral properties and E_a, such that—for example—red-sensitivity would imply a lower energy barrier for activation than blue-sensitivity. This idea has influenced thinking on the ecology of visual pigments for almost half a century[3,9–13] but has been difficult to test experimentally. In nature, the spectral properties of the visual pigment molecules are 'tuned' by at least two different molecular mechanisms: amino-acid substitutions in the protein (opsin) part[14], acting on an evolutionary timescale, or a change of the prosthetic group (the chromophore) in one and the same opsin, effective on a physiological timescale[15]. In vertebrates, the latter mechanism entails a switch between retinaldehyde (retinal A1) and 3-dehydroretinaldehyde (retinal A2), as found in connection with (for example) seasonal or migratory changes in fishes, and in amphibian metamorphosis[15,16]. The A1 → A2 substitution red-shifts the pigment in a regular manner[17]. As all known vertebrate visual-pigment spectra can be described over the main absorption range by either of two universal templates (A1 or A2) with λ_{max} as sole variable[18], a supposed relation between spectral properties and the energy barrier for activation may to a first approximation be treated as a relation between λ_{max} and E_a.

Our primary goal required comparison between two pigments differing significantly in λ_{max} owing to different opsins. For this we studied the pigments of the main rod and cone populations in the

Table 1 Apparent activation energies for visual pigments in six amphibian photoreceptors

Source	Chromophore	λ_{max} (mm)	E_a (kcal mol^{-1})†	Number of points	Number of retinas
Rana temporaria rod	A1	502	45.7 ± 0.4	18	3
Rana temporaria cone	A1	562	45.5 ± 0.4	20	4
Bufo bufo rod	A1	502	49.2 ± 0.6**	21	3
Rana temporaria juv. cone	A2	629	(≤) 40.4 ± 1.6*	9	3
Xenopus laevis rod	A2	528	41.2 ± 1.5*	20	6

Values of the apparent activation energy, E_a, were estimated from equation (1). Statistical significances indicated for rods refer to a comparison with adult frog rods and for the cone A2 pigment to a comparison with its A1 pair. The amino acid sequences of the rod opsins of *Rana temporaria*, *Bufo bufo* and *Xenopus laevis* are compared in ref. 20.
† Values are mean ± s.e.m. Asterisk, $P < 0.05$; two asterisks, $P < 0.01$.

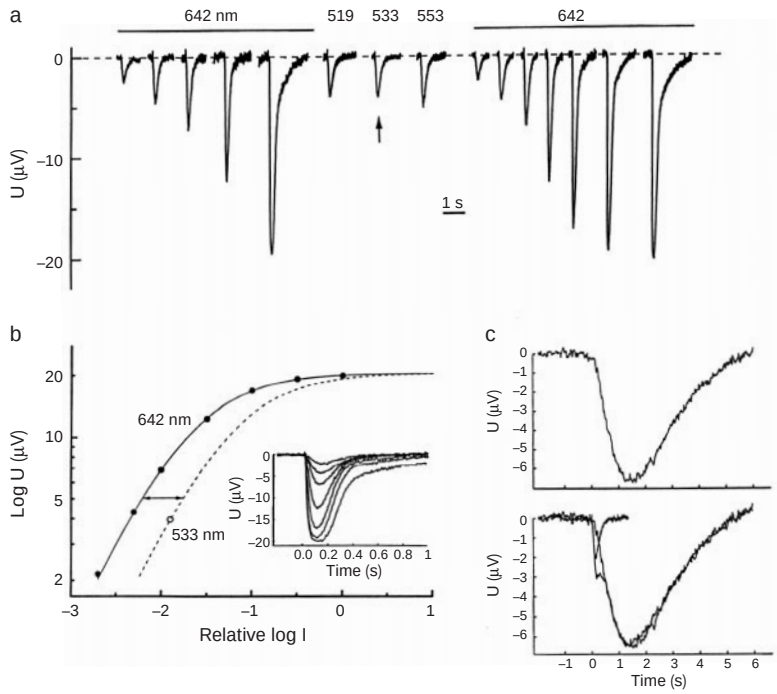

Figure 1 Measurement of spectral sensitivities of rods and cones in the isolated retina. **a**, The protocol for determining spectral sensitivities, exemplified by recordings from cones of the adult frog. Sequences of stimulation with five or seven flash intensities at a reference wavelength (642 nm for cones) were interleaved with series of 3–20 dim flashes at each of 3–5 different test wavelengths. Averaged dim-flash responses are shown for 519, 533 and 553 nm. The timescale bar (1 s) refers to the kinetics of the (arbitrarily spaced) responses. **b**, Response families (inset) recorded at the reference wavelength were used for construction of log (flash intensity) – log (response amplitude) functions (filled circles), described by a Michaelis curve (solid line). Sensitivity at each test wavelength relative to the reference was determined from the required lateral shift of the curve (dashed line); here we show data for the response amplitude measured at 533 nm (open circle). **c**, Isolation of the rod component of mixed responses from the dark-adapted retina. The upper trace is a pure rod response, as obtained at shorter wavelengths (518 nm, single record). The lower trace is a mixed rod/cone response as obtained at long wavelengths (here 720 nm). The rod and cone components can be reliably separated by their kinetics, as shown by the superimposed traces: one reproduces the upper 518-nm trace and the other is a pure cone response to the same 720-nm flash intensity as for the mixed response, but recorded 4 s after a rod-saturating blue pre-flash[19]. Temperature, 25 °C.

adult frog retina, the 'rhodopsin' rods and the 'red' cones (*Rana temporaria*, A1, $\lambda_{max} = 502$ and 562 nm, respectively)[16–19]. Second, we wanted to compare two spectrally similar pigments with different opsins, and for this purpose we included the 'frog-like' rhodopsin of the toad, *Bufo bufo* (A1, $\lambda_{max} = 502$ nm)[18,20]. Third, to compare two pigments differing in λ_{max} due to a chromophore difference alone, we studied the A2 variant of the frog's red-cone pigment ($\lambda_{max} = 629$ nm), which occurs naturally in tadpoles[16]. Spectra were determined from electrophysiologically recorded spectral sensitivities of the respective photoreceptor cells (see Methods and Fig. 1), which is the only way to measure the far red end with high accuracy[18], and has the further advantage that results refer to the functional visual pigment in reasonably natural conditions.

Figure 2a shows average spectral sensitivities of rods and red cones recorded in retinas of adult frogs at 5.4 °C ('cold', denoted C) and 25.0 °C ('warm', denoted W). In both photoreceptor types, relative W sensitivities rise successively above C sensitivities at the longest wavelengths. The sensitivity difference at each wavelength beyond the divergence in the vicinity of 640 nm (on the wavenumber scale, around $(1.6–1.5) \times 10^6\ m^{-1}$) yields one estimate of E_a (equation (1)). The mean ± s.e.m. of the estimates is $E_{ar} = 45.7 \pm 0.4$ kcal mol^{-1} for rods and $E_{ac} = 45.5 \pm 0.4$ kcal mol^{-1} for cones. These s.e.m.s include not only the variability between the point estimates, but also the uncertainty associated with the relative positioning of C and W spectra on the ordinate. The 95% confidence interval for the difference $(E_{ar} - E_{ac})$ is 0.2 ± 1.8 kcal mol^{-1}; that is, only with probability $P < 0.05$ may E_{ac} be more than 4.4% smaller than E_{ar}. The hypothesis that the red shift from the rod to the red cone pigment is wholly due to lowered activation energy requires $E_a \propto 1/\lambda_{max}$, implying that E_{ac} be 10.7% smaller than E_{ar}. This is rejected on the $P < 0.0005$ level.

Results from the spectrally similar rods of toad and frog are compared in Fig. 2b. When the two C spectra, as well as the shorter-wavelength limbs of the two W spectra, are optimally matched, the W data for toad at long wavelengths are seen to lie systematically above those for frog. This suggests that toad rhodopsin has a higher activation energy, and indeed the mean estimates differ significantly ($P < 0.01$; see Table 1). To summarize, two pigments with the same λ_{max} may have different E_a, and two pigments wiht similar E_a may have substantially different λ_{max}. Equal activation energy appears to be neither a necessary nor a sufficient condition for equal λ_{max}.

We show spectra of red cones of *Rana* tadpoles with about 40% A2 in Fig. 3. It may be seen that the temperature effect is much weaker than in Fig. 2. With the given proportion of A2, more than 90% of the threshold response at wavelengths $\lambda > 700$ nm is due to excitations in A2 molecules. Estimation of E_a based on these wavelengths gave 40.4 ± 1.6 kcal mol^{-1} for frog cone opsin with chromophore A2, clearly different from the value for its A1 counterpart ($P < 0.05$). However, the A2 estimate should properly be regarded as an upper bound (see Methods), and the true difference could in fact be greater. For comparison, we studied a spectrally similar A2 pigment in the red cones of adult clawed toad (*Xenopus laevis*, data not shown), finding hints of a temperature effect only from 752 nm (suggesting that $E_a \lesssim 39$ kcal mol^{-1}). A third A2 pigment studied, the 528-nm porphyropsin of *Xenopus* rods (the pair of an A1 rhodopsin at ~502 nm), also gave a low E_a estimate (41.2 ± 1.6 kcal mol^{-1}), supporting the notion of a generic difference between A2- and A1-based pigments.

The results are summarized in Table 1. The activation energies for A1 pigments are in broad agreement with estimates from photocalorimetry on bovine rhodopsin (45–48 kcal mol^{-1}; ref. 21) as well as from bleaching studies on frog and bovine rhodopsin extracts,

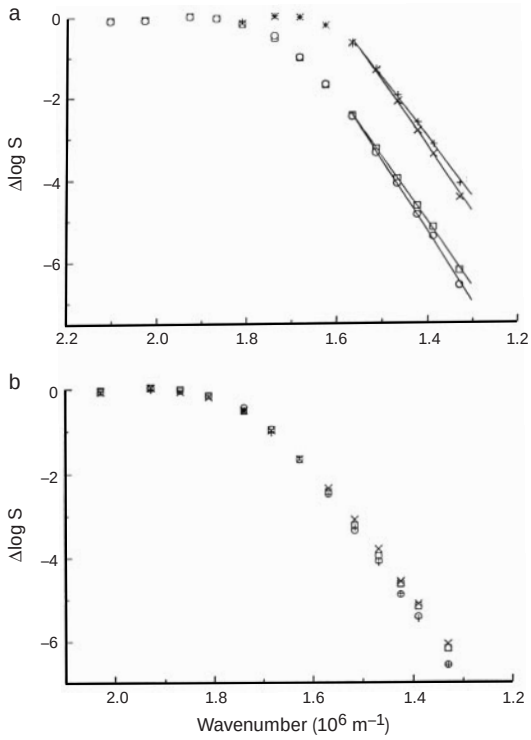

Figure 2 Effect of temperature on sensitivity spectra. **a**, Spectral sensitivities of rods and 'red' cones in the adult frog retina at 5.4 °C ('cold', C) and 25 °C ('warm', W). Symbols: circles, rod-C; squares, rod-W; crosses, cone-C; plus signs, cone-W. The rod spectra show averages from 3 retinas, the cone spectra averages from 4 retinas. Straight lines have been drawn in the long-wavelength region for visual guidance; regression coefficients calculated over the interval 638–752 nm are ($\times 10^{-6}$ m) 17.1 (rod-C), 15.8 (rod-W), 16.1 (cone-C) and 14.5 (cone-W). **b**, Comparison of spectral sensitivities of frog and toad rods. Frog data (circles and squares) are reproduced from **a**. Toad data (averages from 3 retinas) are marked by plus signs (C) and crosses (W). Linear regression coefficients calculated for the toad data over the interval 638–752 nm are 17.1×10^{-6} m (6.9 °C) and 15.9×10^{-6} m (25.8 °C) (lines not shown).

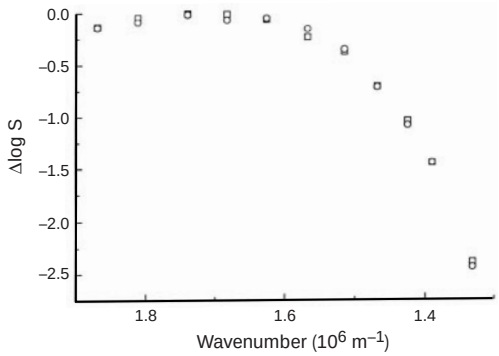

Figure 3 Spectral sensitivities of frog tadpole 'red' cones (circles, 7.9 °C; squares, 24 °C). Averages from 3 retinas. The local slope between the last two points (720–752 nm) is 16.8×10^{-6} m.

whether purely thermal (44 kcal mol^{-1}; ref. 22) or involving combinations of light and heat (44–48.5 kcal mol^{-1}; ref. 1). Lower E_a in A2 pigments is expected *a priori* from the extra C=C bond in the π-electron system of 3-dehydroretinal, and holds as a qualitative rule for pigments in solution[23].

The thermal-energy contribution to visual excitation is functionally important in two respects. First, as shown above, it expands the range of long-wavelength light available for vision. Our results suggest that thermal extension of the spectrum at the red end can be achieved in two ways: either by decreasing the activation energy (as by A1 → A2 substitution), or by increasing the capacity to recruit thermal energy (vibrational modes) towards chromophore isomerization[6]. Second, it implies that pigments may be activated even in the absence of photons. This will cause an intrinsic background 'light' of randomly occurring quantal excitations ('dark events'), which (as they are identical to those due to photons) constitute a type of noise that must necessarily degrade the detectability of real light[24,25]. Improving red-sensitivity by increasing the thermal-energy contribution (regardless by which means) is likely to increase the susceptibility to purely thermal activation. Noise reduction has been proposed to explain the widespread occurrence of visual pigments (or spectral sensitivities) that are blue-shifted relative to the ambient illumination[9–13], including the Purkinje shift from photopic (daylight) vision to relatively short-wavelength-sensitive scotopic (night) vision[3]. In rods, a general correlation between red-sensitivity and high rates of dark events has been experimentally demonstrated[11,12]; this evidence mainly rests on spectral variation associated with chromophore differences. In cones, which offer a wider range of opsin-based spectral variation, the 'dark' noise power of single red cones[26,27], as well as the variability of light detection by the dark-adapted human L + M cone system[28], are consistent with high rates of dark events. (Quantal excitations in cones are too small to be directly recorded.)

We note, however, that our estimates of E_a for A1-based pigments (Table 1) are more than twice those obtained from the temperature dependence of dark-event rates in toad rhodopsin rods[25]. This is consistent with the idea that purely thermal activation occurs by a different molecular route than does activation by photons, even when the latter depends on support from thermal energy[29]. □

Methods

Preparation and recording

Mass photoresponses of rods and cones were recorded as electroretinogram potentials across the isolated retina, superfused and illuminated from the receptor side. Synaptic transmission was blocked by aspartate. Spectral sensitivities were measured with interference filters (Schott DIL or Melles Griot) selected from a complement of 29 individually calibrated filters with peak transmissions covering the range 397–802 nm (in most cases, however, the lamp output and spectral sensitivities of the cells restricted the useful wavelength range to ⩽752 nm). In each experiment at least two spectra were recorded, one ('C') usually at a temperature in the interval 5–8 °C and one ('W') usually at 25–27 °C; the order of W and C was varied between experiments. Temperature was monitored with a thermistor in the bath close to the retina. After dissection and after each temperature change, the retina was allowed to adapt for at least 1 h before recording began. The protocol is shown in Fig. 1. At each wavelength, responses to 3–20 nominally identical 20-ms flashes of dim light were averaged. Possible changes in saturating response amplitude during the experiment were corrected for by linear interpolation between interleaved intensity-response functions recorded with a reference wavelength. Cone responses were isolated either by selective suppression of rods with steady background light (in two of four frog cone experiments in Table 1), or, in the dark-adapted retina, by stimulation at a fixed time after a strong blue pre-flash, while rods were still saturated but cones had essentially recovered[19] (two experiments). Rod responses were recorded in the dark-adapted retina; cone contributions to responses to longer wavelengths were eliminated on the basis of kinetics (Fig. 1c). Distortion by selective absorption in structures other than visual pigment, waveguide properties of photoreceptors, and response contributions from shorter-wavelength-sensitive cone and rod types can be ruled out in the wavelength range used here (near and beyond the peak of rhodopsin rods and 'red' cones), and with the present recording geometry[19]. However, rhodopsin absorbance will affect the shape of both rod and cone spectra, as a virtually full dark-adapted complement of rhodopsin was present throughout all experiments. This will both broaden the peak of rod spectra compared with dilute pigment ('self-screening' with optical density ~0.5)[16,19], and depress apparent cone sensitivities on the short-wavelength side of the peak[19]. But screening by rhodopsin did not change during experiments, as there was no substantial pigment loss by bleaching. In the 'worst' case (cone experiments with a continuous rod-depressing background), the bleaching velocity was 1% per 30 min; the isolated retina is known to possess a sufficient capacity for pigment regeneration to compensate for this completely over at least 5 h. Screening is unimportant in the long-wavelength range, where rhodopsin absorbance is low. See refs 19 and 30 for further technical details.

Analysis

At each wavelength, the log sensitivity (log *S*) difference compared with a reference wavelength was determined. All differences were expressed relative to log peak sensitivity (= 0) and these normalized values of log*S* for each wavelength were averaged across

experiments for each photoreceptor type, C and W separately. The optimal relative positioning along the log$S$ axis of the averaged C and W spectra for each photoreceptor type was found by minimizing the sum of squares (SS) of the differences between C and W points at 'shorter' wavelengths (below hc/E_a, determined by iteration). The least SS, denoted SS_μ, provides directly a statistical measure of the 'matching' uncertainty connected with the vertical alignment (see below). The sensitivity values of the averaged spectra under the optimal match are denoted $\Delta\log S$. The difference $\Delta\log S_{Wi} - \Delta\log S_{Ci}$ recorded at each 'long' wavelength λ_i was converted into its photon energy equivalent through the equation[2,5–7].

$$hc/\lambda_a = E_a = hc/\lambda_i + (hc/T)[-\partial\log S/\partial(1/T)]_i/[\partial\log S/\partial(1/\lambda)]_i \quad (1)$$

For the calculations, $[-\partial\log S/\partial(1/T)] = (\Delta\log S_{Wi} - \Delta\log S_{Ci})/(1/T_C - 1/T_W)$, $T = T_C$, and $[\partial\log S/\partial(1/\lambda)]_i$ is the local slope of the C-spectrum at λ_i, taken as the mean of $(\Delta\log S_{C(i-1)} - \Delta\log S_{C(i)})/(1/\lambda_{i-1} - 1/\lambda_i)$ and $(\Delta\log S_{Ci} - \Delta\log S_{C(i+1)})/(1/\lambda_i - 1/\lambda_{i+1})$. (For the largest λ_i, the slope from λ_{i-1} to λ_i was accepted as such.)

The statistical error of the estimate depends on two variance components. (1) Variance connected with the overall vertical matching of C and W spectra was estimated by a 'matching' mean square $s_\mu^2 = A_{max}SS_\mu/(m-1)$. Here A_{max} is the largest value of the energy conversion factor $hc/[(1 - T_C/T_W)\partial\log S_C/\partial(1/\lambda)_i]$ in that data set (corresponding to the smallest local slope), SS_μ is as defined earlier, and m is the number of (shorter-wavelength) data point pairs used for the matching. (2) Variance between the point estimates of E_a under a fixed C-W match was estimated by a conventional 'sample' mean square $s_\rho^2 = SS_\rho/(M-1)$. Here, SS_ρ is the sum of squares of the sample and M is sample size, that is, the number of (longer-wavelength) data point pairs used for estimation. Since C-W matching and E_a estimation were based on non-overlapping data sets, the estimator of total variance (denoted s_E^2) is a sum of s_μ^2 and s_ρ^2, weighted by their respective degrees of freedom ($df_\mu = m - 1$ and $df_\rho = M - 1$). The total s.e.m. is $= s_E/\sqrt{M}$. Confidence limits and statistical significance testing were based on Student's t-test with degrees of freedom according to the appropriate variance measure in each case.

The validity of equation (1) depends on the existence of the true positive differences $\Delta\log S_W - \Delta\log S_C$. Otherwise (for random, zero or negative differences) no definite values for E_a can be obtained, only an upper limit ($E_a \leqslant hc/\lambda_i$). In the case of frog tadpole cones only three wavelengths were available for estimation (Fig. 3), and there is the possibility that the small differences observed reflect essentially random variation; hence, the corresponding estimate in Table 1 should be regarded as an upper bound. In *Xenopus* red cones, temperature effects were even less reliable.

For determining the A1/A2 ratio in A2-containing photoreceptors, a curve-fitting program was used where given proportions of A1 and A2 templates (recently tuned for best fit to a large body of spectral data)[18] are added together, while the λ_{max} difference within an A1–A2 pair is constrained to obey the Dartnall–Lythgoe relation[17]. (Description of the shape of our spectra with templates for absorbance of dilute pigment requires rhodopsin screening be taken into account; see above.) In our adult *Xenopus*, we detected no A1 chromophore, while the *Rana* tadpoles were found to have approximately a 0.6/0.4 mixture of A1 and A2. The program was also used to analyse the expected contribution of the 562-nm A1 component to the sensitivity of these tadpole cones at different wavelengths. Only the longest wavelengths, with less than 8% contribution from A1, were used in determining E_a for the A2 pigment.

Received 16 March; accepted 2 November 1999.

1. St George, R. C. C. The interplay of light and heat in bleaching rhodopsin. *J. Gen. Physiol.* **35,** 495–517 (1952).
2. Stiles, W. S. in *Trans. of the Optical Convention of the Worshipful Company of Spectacle Makers* 97–107 (Spectacle Makers' Co., London, 1948).
3. Barlow, H. B. Purkinje shift and retinal noise. *Nature* **179,** 255–256 (1957).
4. de Vries, H. Der Einfluss der Temperatur des Auges auf die spektrale Empfindlichkeitskurve. *Experientia* **4,** 357–358 (1948).
5. Denton, E. J. & Pirenne, M. H. The visual sensitivity of the toad *Xenopus laevis*. *J. Physiol.* **125,** 181–207 (1954).
6. Lewis, P. R. A theoretical interpretation of spectral sensitivity curves at long wavelengths. *J. Physiol.* **130,** 45–52 (1955).
7. Srebro, R. A thermal component of excitation in the lateral eye of *Limulus*. *J. Physiol.* **187,** 417–425 (1966).
8. Lamb, T. D. Effects of temperature changes on toad rod photocurrents. *J. Physiol.* **346,** 557–578 (1984).
9. Lythgoe, J. N. in *Sensory Biology of Aquatic Animals* (eds Atema, J., Fay, R. R., Popper, A. N. & Tavolga, W. N.) 57–82 (Springer, New York, 1988).
10. Goldsmith, T. H. in *Facets of Vision* (eds Stavenga, D. G. & Hardie, R. C.) 1–14 (Springer, Berlin, 1989).
11. Donner, K., Firsov, M. L. & Govardovskii, V. I. The frequency of isomerization-like "dark" events in rhodopsin and porphyropsin rods of the bullfrog retina. *J. Physiol.* **428,** 673–692 (1990).
12. Firsov, M. L. & Govardovskii, V. I. Dark noise of visual pigments with different absorption maxima. *Sensornye Sistemy* **4,** 25–34 (1990). (In Russian).
13. Bowmaker, J. K. *et al.* Visual pigments and the photic environment: The cottoid fish of Lake Baikal. *Vision Res.* **34,** 591–606 (1994).
14. Neitz, M., Neitz, J. & Jacobs, G. H. Spectral tuning of pigments underlying red–green color vision. *Science* **252,** 971–974 (1991).
15. Bridges, C. D. B. in *Handbook of Sensory Physiology* Vol. VII/1 (ed. Dartnall, H. J. A.) 417–480 (Springer, Berlin, 1972).
16. Reuter, T. Visual pigments and ganglion cell activity in the retinae of tadpoles and adult frogs (*Rana temporaria* L.). *Acta Zool. Fenn.* **122,** 1–64 (1969).
17. Dartnall, H. J. A. & Lythgoe, J. N. The spectral clustering of visual pigments. *Vision Res.* **5,** 81–100 (1965).
18. Govardovskii, V. I., Fyhrquist, N., Reuter, T., Kuzmin, D. G. & Donner, K. In search of the visual pigment nomogram. *Vis. Neurosci.* (in the press).
19. Koskelainen, A., Hemilä, S. & Donner, K. Spectral sensitivities of short- and long-wavelength sensitive cone mechanisms in the frog retina. *Acta Physiol. Scand.* **152,** 115–124 (1994).
20. Fyhrquist, N. *et al.* Rhodopsins from three frog and toad species: sequences and functional comparisons. *Exp. Eye Res.* **66,** 295–305 (1998).
21. Cooper, A. Energy uptake in the first step of visual excitation. *Nature* **282,** 531–533 (1979).
22. Lythgoe, R. J. & Quilliam, J. P. The thermal decomposition of visual purple. *J. Physiol.* **93,** 24–38 (1938).
23. Williams, T. P. & Milby, S. E. The thermal decomposition of some visual pigments. *Vision Res.* **8,** 359–367 (1968).
24. Barlow, H. B. Retinal noise and absolute threshold. *J. Opt. Soc. Am.* **46,** 634–639 (1956).
25. Baylor, D. A., Matthews, G. & Yau, K.-W. Two components of electrical dark noise in toad retinal rod outer segments. *J. Physiol.* **309,** 591–621 (1980).
26. Lamb, T. D. & Simon, E. J. Analysis of electrical noise in turtle cones. *J. Physiol.* **272,** 435–468 (1977).
27. Schnapf, J. L., Nunn, B. J., Meister, M. & Baylor, D. A. Visual transduction in cones of the monkey *Macaca fascicularis*. *J. Physiol.* **427,** 681–713 (1990).
28. Donner, K. Noise and the absolute thresholds of cone and rod vision. *Vision Res.* **32,** 853–866 (1992).
29. Barlow, R. B., Birge, R. R., Kaplan, E. & Tallent, J. R. On the molecular origin of photoreceptor noise. *Nature* **366,** 64–66 (1993).
30. Donner, K., Hemilä, S. & Koskelainen, A. Light adaptation of cone photoresponses studied at the photoreceptor and ganglion cell levels in the frog retina. *Vision Res.* **38,** 19–36 (1998).

Acknowledgements

We thank V. I. Govardovskii for the nomogram-fitting program used for spectral analysis of pigments, H. Rita for statistical advice, C. Haldin and S. Pietilä for technical assistance, T. Reuter for comments on the manuscript, and Kilpisjärvi Biological Station for providing experimental animals. This work was supported by the Academy of Finland and by the Finnish Graduate Schools of Neuroscience and of Molecular Nanotechnology.

Correspondence and requests for materials should be addressed to A.K. (e-mail: ari.koskelainen@hut.fi).

Bioorganic synthesis of lipid-modified proteins for the study of signal transduction

Benjamin Bader*, Karsten Kuhn*†, David J. Owen*†‡, Herbert Waldmann*†, Alfred Wittinghofer* & Jürgen Kuhlmann*

** Max-Planck Institut für Molekulare Physiologie, Otto Hahn Strasse 11, 44227 Dortmund, Germany*
† Universität Dortmund, FB 3, Organische Chemie, Otto Hahn Strasse 11, 44227 Dortmund, Germany

Biological membranes define the boundaries of the cellular compartments in higher eukaryotes and are active in many processes such as signal transduction and vesicular transport. Although post-translational lipid modification of numerous proteins in signal transduction is crucial for biological function[1], analysis of protein–protein interactions has mainly focused on recombinant proteins in solution under defined *in vitro* conditions. Here we present a new strategy for the synthesis of such lipid-modified proteins. It involves the bacterial expression of a carboxy-terminally truncated non-lipidated protein, the chemical synthesis of differently lipidated peptides representing the C terminus of the proteins, and their covalent coupling. Our technique is demonstrated using Ras constructs, which exhibit properties very similar to fully processed Ras, but can be produced in high yields and are open for selective modifications. These constructs are operative in biophysical and cellular assay systems, showing specific recognition of effectors by Ras lipoproteins inserted into the membrane surface of biosensors and transforming activity of oncogenic variants after microinjection into cultured cells.

Ras, a GTP-binding protein involved in signal transduction[2], has to undergo several post-translational lipid-modification steps as a crucial prerequisite for biological activity[3]. The most important

‡ Current address: Department of Medicinal Chemistry, Victorian College of Pharmacy, 381 Royal Parade, Parkville, Victoria 3052, Australia.